Polymers **2013**, *5*, 696-705; doi:10.3390/polym5020696

OPEN ACCESS

polymers

ISSN 2073-4360

www.mdpi.com/journal/polymers

Article

Ion Permeability of Free-Suspended Layer-by-Layer (LbL) Films Prepared Using an Alginate Scaffold

Katsuhiko Sato, Takuto Shiba and Jun-ichi Anzai *

Graduate School of Pharmaceutical Sciences, Tohoku University; Aramaki, Aoba-ku, Sendai 980-8578, Japan; E-Mails: satok@m.tohoku.ac.jp (K.S.); b1ym1015@s.tohoku.ac.jp (T.S.)

* Author to whom correspondence should be addressed; E-Mail: junanzai@mail.pharm.tohoku.ac.jp; Tel.: +81-22-795-6841; Fax: +81-22-795-6840.

Received: 26 March 2013; in revised form: 9 May 2013 / Accepted: 3 June 2013 / Published: 6 June 2013

Abstract: Layer-by-layer (LbL) films were prepared over an aperture (diameter 1–5 mm) on a glass plate to study ion permeation across free-suspended LbL films. LbL films were prepared by depositing alternating layers of poly(allylamine hydrochloride) (PAH) and poly(styrene sulfonate) (PSS) on the surface of a glass plate with an aperture filled with an alginate gel, followed by dissolution of the alginate gel. PAH-PSS films prepared in this way showed permeability to inorganic salts, depending on the size and charge. Permeability to alkali metal chlorides depended on the Stokes radius of the alkali metal cations. The effect of the type of halide was negligible because of the halides' smaller ionic radii. Permeation of multivalent ions such as $Ru(NH_3)_6^{3+}$ and $[Fe(CN)_6]^{3-}$ was severely suppressed owing to Donnan exclusion.

Keywords: layer-by-layer film; free-suspended LbL film; ion permeability; Donnan exclusion

1. Introduction

Much attention has been devoted to the development of polyelectrolyte layer-by-layer (LbL) films in polymer science and technology. LbL thin films can be prepared by alternating deposits of polymeric materials through the electrostatic forces of attraction, hydrogen bonding, and biological affinity [1–4]. The polymeric materials employed for this purpose include synthetic polymers and

nanotubes [5,6], proteins [7,8], and polysaccharides [9,10]. LbL films have been used for constructing molecular architectures [11–13], stimuli-sensitive systems [2,14–17], optical and electrochemical devices [5,10,18–22], and controlled release systems [23–28].

The construction of separation and purification membranes for ions and molecules has also been studied using LbL films and related systems [29–32]. LbL films composed of poly(allylamine hydrochloride) (PAH) and poly(styrene sulfonate) (PSS), which were deposited on the surface of porous supports (pore diameter 20–200 nm), exhibited a high flux of monovalent ions while the flux of multivalent ions was significantly suppressed as a result of enhanced Donnan exclusion, as well as hindered diffusion in the film [33–35]. The selective permeation of organic compounds has also been reported [31]. These results suggest that LbL films hold promise for future application to selective separator layers. Previously, LbL films were deposited on solid supports with micro-pores to study their permeability due to their fragile nature [33,34]. However, evaluation of the ion permeability of support-free LbL films would be of significant importance. In this context, Ono and Decher recently prepared free-standing LbL films composed of PAH and PSS using a decomposable sacrificial thin layer consisting of poly(acrylic acid) (PAA) and poly(ethylene glycol) (PEG) [36]. Robust LbL films can be produced by cross-linking polymer chains [37]. However, the ion permeability of such free-standing LbL films has not yet been evaluated, probably due to their fragility. We recently prepared LbL films on the surface of glass supports with 1 or 3 mm apertures and reported the preliminary results of the ion permeability of the films [38]. The effective surface area of the LbL films was significantly higher than that of LbL films deposited on porous supports. In the present paper, we report the permeability of alkali metal halides across free-suspended PAH-PSS films, which were prepared using an alginate scaffold. We found size- and charge-dependent permeability of alkali metal halides across the free-suspended PAH-PSS films.

2. Experimental Section

2.1. Materials

An aqueous solution (20%) of poly(allylamine hydrochloride) [PAH; MW, ~150,000] was obtained from Nitto Bouseki Co. (Tokyo, Japan). Poly(styrene sulfonate) [PSS; MW, ~5,000,000] was purchased from Scientific Polymer Products, Inc. (New York, NY, USA). Sodium alginate (ALG) was purchased from Sigma-Aldrich Co. (St. Loius, MO, USA). Fluorescein-modified PAH (F-PAH) was synthesized from the reaction of 100 mg PAH and 16.2 mg fluoresceinisothiocyanate, as previously reported (about 3 mol % amino groups in PAH were modified by a fluorescein residue, as determined by UV-visible spectrometry) [39]. All other reagents used were of the highest grade available.

2.2. Preparation of LbL Films

LbL films were prepared using a glass disk (diameter, 20 mm; thickness, 1 mm) with an aperture of diameter, 1, 3, or 5 mm. The aperture of the glass disk was filled with an ALG gel as the scaffold was prepared from a mixture of 2% ALG solution and 10% $CaCl_2$ solution. The ALG gel-filled glass disk was then immersed in 2 mg/mL PAH solution (0.1 M Tris-HCl buffer containing 1% $CaCl_2$, pH 7.0) for 15 min to cover the ALG gel surface with a PAH layer through electrostatic affinity, and rinsed in

working buffer for 5 min. In a similar manner, the next PSS layer was deposited on the ALG gel by immersing the PAH-covered ALG gel in 2 mg/mL PSS solution (0.1 M Tris-HCl buffer containing 1% $CaCl_2$, pH 7.0) for 15 min and rinsing in the working buffer for 5 min. Alternate deposits of PAH and PSS layers were used to construct LbL films with the desired number of layers. It is noted here that PAH and PSS solutions used contained 1% $CaCl_2$ to keep the ALG gel stable. Added $CaCl_2$ did not affect undesirable effect on the film deposition. The glass disk was then immersed in 0.2 M ethylenediaminetetraacetic acid solution for 30 min to dissolve the ALG scaffold [39]. Finally, the LbL film deposited on one side of the glass disk was carefully removed. The procedure for preparing free-suspended LbL film was schematically illustrated in our previous paper [38].

2.3. Absorption Spectra of LbL Films

F-PAH-PSS LbL films were prepared in a similar manner on a glass plate ($1 \times 9 \times 40$ mm^3) with an aperture (diameter 5 mm) for recording the absorption spectra. One side of the glass plate was coated with black paint, prior to use to block out incidental light so that the absorption spectrum of the LbL films located over the aperture was recorded accurately. The absorption spectra of LbL films were recorded in 0.1 M Tris-HCl buffer containing 1% $CaCl_2$, pH 7.0, using a UV-visible absorption spectrophotometer (UV-3100PC, Shimadzu Co., Kyoto, Japan).

2.4. Ion Permeation

Figure 1 shows the apparatus used for measuring ion permeation. One of the chambers contained salt solution (50 mL, source phase) and the other chamber was filled with distilled water (50 mL, receiving phase). Both solutions in the source and receiving phases contained only salts to be transported, except for the solutions used for evaluating the effects of pH. The concentration of salt transported across the film was estimated by the conductivity of the solution in the receiving phase using a conductivity cell (3552-10D, Horiba Co., Kyoto, Japan). Both source and receiving phase solutions were gently stirred to minimize concentration polarization at the film-solution interfaces. The effect of osmotic flow on the solution volume was negligible under the experimental conditions. All measurements were carried out under ambient temperature (*ca.* 20 °C).

Figure 1. U-shaped glass cell for measuring ion permeation: (**A**) Source phase (50 mL); (**B**) Receiving phase (50 mL); (**C**) Conductivity cell. A conductivity cell was immersed in the receiving phase to monitor the concentration of salt transported.

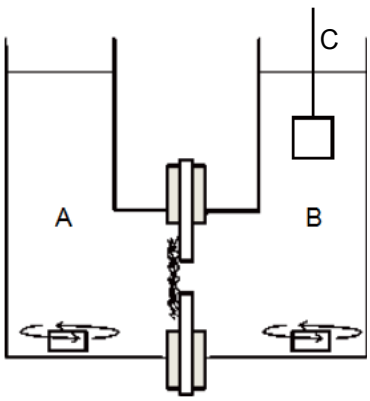

3. Results and Discussion

3.1. Preparation of Free-Suspended LbL Film

The free-suspended LbL films were prepared on the glass disk with a 5 mm aperture using F-PAH and PSS, and UV-visible absorption spectra were measured (Figure 2). The films exhibited absorption maxima around 500 nm originating from a fluorescein moiety in F-PAH. The intensity of the peaks increased with increasing number of deposits, suggesting that F-PAH and PSS were successfully deposited in a layer-by-layer fashion. The film deposition was visualized more clearly in UV-visible absorption spectra using F-PAH, as compared with monitoring based on the absorption of PSS [40]. A similar result has been previously reported for LbL films prepared over a 1 mm aperture [38]. The deposition of at least three bilayers, $(F\text{-}PAH\text{-}PSS)_3$, was a prerequisite for constructing free-suspended LbL film due to the fragility of the thinner films. Figure 3 shows photographs of the glass disk with a 5 mm aperture before and after formation of PAH-PSS film. These data clearly show that free-suspended LbL films composed of PAH and PSS can be prepared by the present protocol.

Figure 2. Absorption spectra of layer-by-layer (LbL) films composed of Fluorescein-modified-poly(allylamine hydrochloride) (F-PAH) and poly(styrene sulfonate) (PSS). The number of (F-PAH-PSS) bilayers: (**a**) 3; (**b**) 5; (**c**) 7; (**d**) 10; and (**e**) 0 (film-free glass disk).

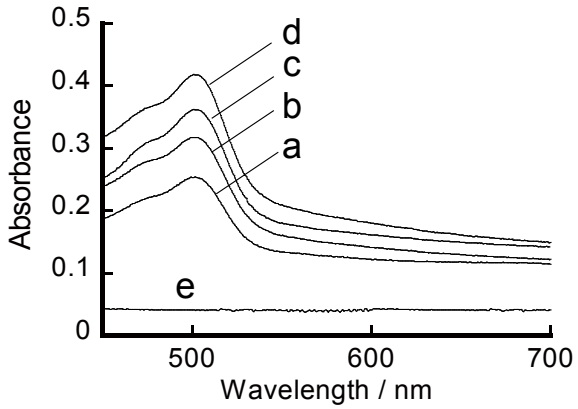

Figure 3. Photographs of a glass disk with a 5 mm aperture (**a**) before and (**b**) after $(PAH\text{-}PSS)_5$ film formation.

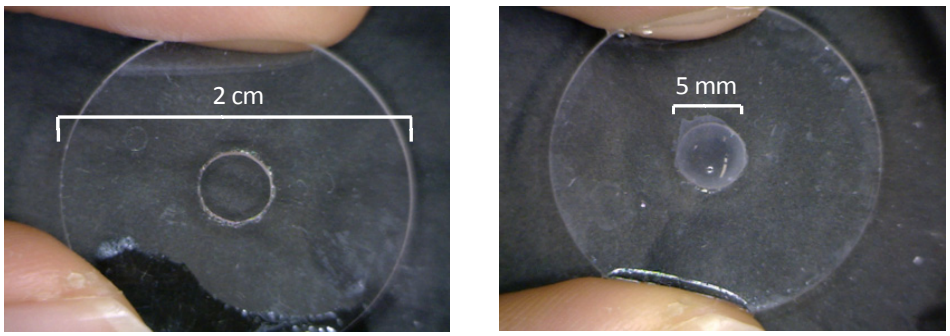

3.2. Ion Permeation

The U-shaped glass cell illustrated in Figure 1 was used to evaluate the ion permeability of free-suspended LbL films. The concentration of salts in the receiving phase was monitored by conductivity changes in the solution. We found that the conductivity of the receiving phase increased linearly with increasing time in all cases, showing that salt concentration in the receiving phase increased linearly with time. This implies that changes in the salt concentration in the source phase were negligible during the measurements. In fact, judging from the conductivity, less than 2.5 μmol of ions was transported across the film within the experimental time scale (*i.e.*, 120 min), which corresponds to *ca.* 0.05% of the amount of salts added to the source phase. Consequently, we were able to estimate the ion permeability of the salts across the LbL film from the slope of a linear plot of salt concentration in the receiving phase *vs.* time.

Figure 4 shows the permeability of alkali chlorides across $(PAH\text{-}PSS)_5$ and $(PAH\text{-}PSS)_5PAH$ films (film diameter, 1 mm). The permeability of alkali chlorides increased in the order of LiCl < NaCl < KCl < RbCl < CsCl for both the $(PAH\text{-}PSS)_5$ and $(PAH\text{-}PSS)_5PAH$ films, suggesting the size of alkali metal cations plays a key role. The result shows that alkali metal chlorides, consisting of cations with smaller Stokes radii, are transported faster than salts with cations of larger Stokes radii. Stokes radii of alkali metal cations were reported to be in the order of $Cs^+ \leq Rb^+ < K^+ < Na^+ < Li^+$ [41,42]. A similar trend in the permeability of alkali metal chlorides has been reported for poly(vinylamine)-PSS LbL films deposited on a porous support [43].

Figure 4. Permeability of alkali chlorides across $(PAH\text{-}PSS)_5$ (open column) and $(PAH\text{-}PSS)_5PAH$ films (filled column) with a 1 mm diameter. The average values for the three measurements are reported.

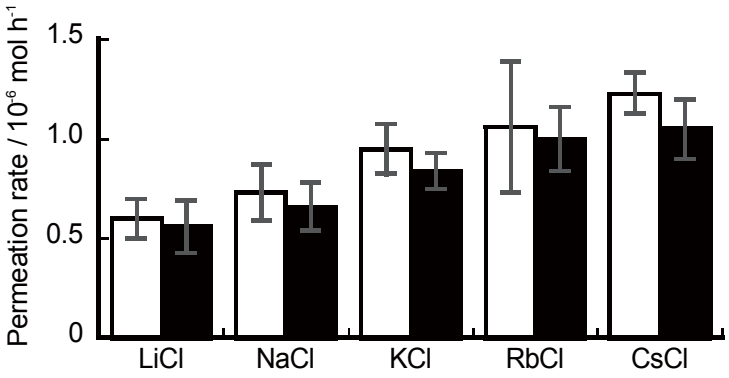

The permeability of NaCl, NaBr, and NaI was measured in a similar way to evaluate the effects of type of anionic species. Figure 5 shows permeability of the salts across $(PAH\text{-}PSS)_5$ and $(PAH\text{-}PSS)_5PAH$ films. The permeation rates of the salts were in the range of $(0.73 - 0.85) \times 10^{-6}$ and $(0.64 - 0.80) \times 10^{-6}$ mol h^{-1} for $(PAH\text{-}PSS)_5$ and $(PAH\text{-}PSS)_5PAH$ films, respectively. Thus, permeability did not depend on the type of anion because the anions had smaller Stokes radii compared with the Na^+ ions [41,42]. These results also support the view that the permeation rate of alkali chlorides depends on the Stokes radii of the cationic species. It has been reported that NaCl, NaBr, and NaI exhibit comparable permeability across LbL films deposited on a porous support [44].

Figure 5. Permeability of alkali halides across $(PAH\text{-}PSS)_5$ (open column) and $(PAH\text{-}PSS)_5PAH$ films (filled column) with 1 mm diameter. The average values of three measurements are reported.

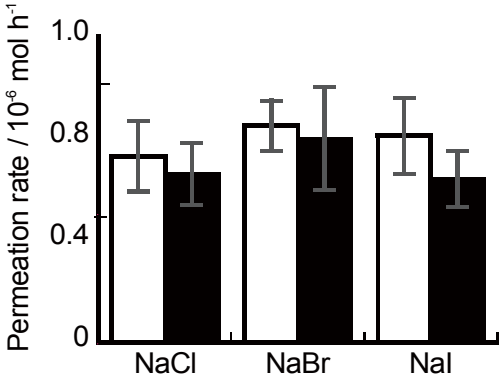

For all salts tested, average values in the permeation rate for $(PAH\text{-}PSS)_5$ film were slightly higher than those for $(PAH\text{-}PSS)_5PAH$ film. The suppressed permeation of the $(PAH\text{-}PSS)_5PAH$ film may be related to Donnan exclusion of the cations at the positively charged surface due to PAH and/or enhanced film thickness by the addition of a terminal PAH layer. Thus, one possible barrier to ion permeation across the LbL film may be due to Donnan exclusion of the ions at the surface of the film because the outermost surface always contains excess charge. It is likely that alkali metal cations undergo Donnan exclusion at the positively charged surface of the $(PAH\text{-}PSS)_5PAH$ film, resulting in suppressed permeation. To verify the effects of the surface charge of the film, the permeability of NaCl was measured across $(PAH\text{-}PSS)_5$ and $(PAH\text{-}PSS)_5PAH$ films at pH 4.0, 7.0, and 9.0. The density of the positive charges on the surface of $(PAH\text{-}PSS)_5PAH$ film would depend on the pH of the solution because the amount of positive charge on the outermost PAH layer depends on the environmental pH. It has been reported that the degree of protonation of PAH chains in PAH-poly(methacrylic acid) complex is about 0.75, 0.50, and 0.45 at pH 4.0, 7.0, and 9.0, respectively [45]. Figure 6 shows the pH-dependent permeation of NaCl across LbL films. The permeability of NaCl across the $(PAH\text{-}PSS)_5PAH$ film was significantly lower at levels of pH 4.0 than at pH 7.0 and 9.0. These results suggest that Na^+ cations undergo Donnan exclusion more effectively at acidic pH, where PAH chains are highly protonated on the film surface. In contrast, NaCl permeation across $(PAH\text{-}PSS)_5$ film was suppressed to a lesser extent in acidic pH. This is probably due to the enhanced protonation of PAH chains located in the film interior, which would disturb the diffusion of Na^+ ions in the film. These results demonstrated that the surface charge has a significant role in determining the permeability of salts.

To characterize further the effects of Donnan exclusion, the permeability of $[Ru(NH_3)_6]Cl_3$ and $K_3[Fe(CN)_6]$ across $(PAH\text{-}PSS)_5$ and $(PAH\text{-}PSS)_5PAH$ films was compared. The effects of Donnan exclusion may be more clearly observed for multivalent ions. Figure 7 shows the permeability of the salts across the films. The permeability of $[Ru(NH_3)_6]Cl_3$ across $(PAH\text{-}PSS)_5$ film was higher than that across $(PAH\text{-}PSS)_5PAH$ film. On the other hand, the opposite trend was observed for $K_3[Fe(CN)_6]$, suggesting that the surface charge of the LbL film had a predominant effect. It is reasonable to assume that $Fe(CN)_6^{3-}$ ions undergo significant Donnan exclusion at the negatively charged surface of the $(PAH\text{-}PSS)_5$ film. The addition of a terminal PAH layer cancelled the Donnan effect, resulting in

enhanced permeability of $Fe(CN)_6^{3-}$ ions. Harris and coworkers also reported that Donnan exclusion played a significant role in ion transport across LbL films prepared on porous supports [33].

Figure 6. Efects of pH on the permeability of NaCl across $(PAH\text{-}PSS)_5$ (open column) and $(PAH\text{-}PSS)_5PAH$ films (filled column) with a 3 mm diameter. The average values of three measurements are reported.

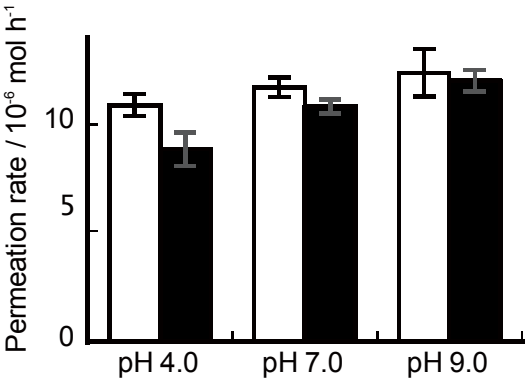

Figure 7. Permeability of $[Ru(NH_3)_6]Cl_3$ and $K_3[Fe(CN)_6]$ across $(PAH\text{-}PSS)_5$ (open column) and $(PAH\text{-}PSS)_5PAH$ films (filled column) with 1 mm diameter. The average values of three measurements are reported.

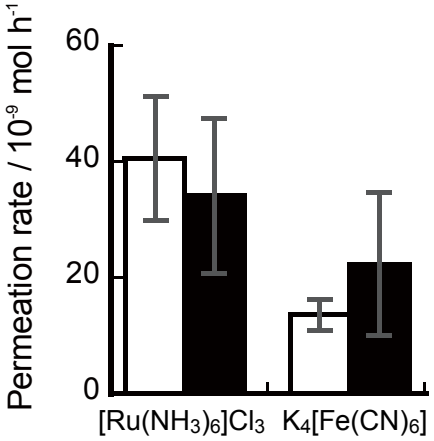

4. Conclusions

We have demonstrated that free-suspended LbL films with 1, 3, and 5 mm diameters can be prepared using ALG gel scaffold. The LbL films exhibited higher permeability to alkali metal cations with smaller Stokes radii. The surface charge of the films significantly affected the permeation rates of salts. The results can be rationalized by the suppressed permeation of ions with the same charge, owing to Donnan exclusion. Thus, the free-suspended LbL films prepared in this study exhibited similar ion permeability as LbL films deposited on a porous support. The protocol reported here would be useful for the construction of LbL films for selective layers in sensors and separators without porous supports. The mechanical fragility of the free-suspended films may be improved by cross-linking the polymer chains for the practical use of the films.

Acknowledgments

This work was supported in part by JSPS KAKENHI Grant Number 24390006.

Conflict of Interest

The authors declare no conflict of interest.

References

1. Decher, G. Fuzzy nanoassemblies: Toward layered polymeric multicomposites. *Science* **1997**, *277*, 1232–1237.
2. Sukhishvili, S.A. Responsive polymer films and capsules via layer-by-layer assembly. *Curr. Opin. Colloid Interface Sci*. **2005**, *10*, 37–44.
3. Tang, Z.; Wang, Y.; Podasiadlo, P.; Kotov, N.A. Biomedical applications of layer-by-layer assemblies: From biomimetics to tissue engineering. *Adv. Mater.* **2006**, *18*, 3203–3224.
4. Marchenko, I.; Yashchenok, A.; German, S.; Inozemtseva, O.; Dorin, D.; Bukreeva, T.; Möhwald, H.; Skirtach, A. Polyelectrolytes: Influence on evaporative self-assembly of particles and assembly of multilayers with polymers, nanoparticles and carbon nanotubes. *Polymers* **2010**, *2*, 690–708.
5. Iost, R.M.; Crespilho, F.N. Layer-by-layer self-assembly and electrochemistry: Applications in biosensing and bioelectronics. *Biosens. Bioelectron*. **2012**, *31*, 1–10.
6. Tomita, S.; Sato, K.; Anzai, J. Layer-by-layer assembled thin films composed of carboxyl-terminated poly(amidoamine) dendrimers as a pH-sensitive nano-device. *J. Colloid Interface Sci*. **2008**, *326*, 35–40.
7. Dai, Z.; Wilson, J.T.; Chaikof, E.L. Construction of pegylated multilayer architectures via (strept)avidin/biotin interactions. *Mater. Sci. Eng. C* **2007**, *27*, 402–408.
8. Hoshi, T.; Akase, S.; Anzai, J. Preparation of multilayer thin films containing avidin through sugar-lectin interactions and their binding properties. *Langmuir* **2002**, *18*, 7024–7028.
9. Crouzier, T.; Boudou, T.; Picart, C. Polysaccharide-based polyelectrolyte multilayers. *Curr. Opin. Colloid Interface Sci*. **2010**, *15*, 417–426.
10. Wang, B.; Anzai, J. Redox reactions of ferricyanide ions in layer-by-layer deposited polysaccharide films: A significant effect of the type of polycation in the films. *Langmuir* 2007, *23*, 7378–7384.
11. Lynn, D.M. Peeling back the layers: Controlled erosion and triggered disassembly of multilayered polyelectrolyte thin films. *Adv. Mater.* **2007**, *19*, 4118–4230.
12. Liu, L.; Chen, Z.; Yang, S.; Jin, X.; Lin, X. A novel inhibition biosensor constructed by layer-by-layer technique based on biospecific affinity for the determination of sulfide. *Sens. Actuators B* **2008**, *129*, 218–224.
13. Takahashi, S.; Sato, K.; Anzai, J. Layer-by-layer construction of protein architectures through avidin-biotin and lectin-sugar interactions for biosensor applications. *Anal. Bioanal. Chem*. **2012**, *402*, 1749–1758.

14. Sato, K.; Kodama, D.; Naka, Y.; Anzai, J. Electrochemically induced disintegration of layer-by-layer-assembled thin films composed of 2-iminobiotin-labeled poly(ethyleneimine) and avidin. *Biomacromolecules* **2006**, *7*, 3302–3305.
15. Inoue, H.; Anzai, J. Stimuli-sensitive thin films prepared by a layer-by-layer deposition of 2-iminobiotin-labeled poly(ethyleneimine) and avidin. *Langmuir* **2005**, *21*, 8354–8359.
16. Wood, K.C.; Zacharie, N.S.; Schmidt, D.J.; Wrightman, S.N.; Andaya, B.J.; Hammond, P.T. Electroactive controlled release thin films. *Proc. Natl. Acad. Sci*. *USA* **2008**, *105*, 2280–2285.
17. Esser-Kahn, A.P.; Odom, S.A.; Sottos, N.R.; White, S.R.; Moore, J.S. Triggered release from polymer capsules. *Macromolecules* **2011**, *44*, 5539–5553.
18. Liu, A.; Anzai, J. Ferrocene-containing polyelectrolyte multilayer films: Effects of electrochemically inactive surface layers on the redox properties. *Langmuir* **2003**, *19*, 4043–4046.
19. Boulmedais, F.; Tang, C.S.; Keller, B.; Vörös, J. Controlled electrodissolution of polyelectrolyte multilayers: A platform technology toward the surface-initiated delivery of drugs. *Adv. Funct. Mater*. **2006**, *16*, 63–70.
20. Lutkenhaus, J.L.; Hammond, P.T. Electrochemically enabled polyelectrolyte multilayer devices: From fuel cells to sensors. *Soft Matter* **2007**, *3*, 804–816.
21. Haiyun, L.; Hu, N. Salt-induced swelling and electrochemical property change of hyaluronic acid/myoglobin multilayer films. *J. Phys. Chem*. **2007**, *111*, 1984–1993.
22. Egawa, Y.; Seki, T.; Takahashi, S.; Anzai, J. Electrochemical and optical sugar sensors based on phenylboronic acid and its derivatives. *Mater. Sci. Eng. C* **2011**, *31*, 1257–1264.
23. Nolan, C.M.; Serpe, M.J.; Lyon, L.A. Thermally modulated insulin release from microgel thin films. *Biomacromolecules* **2004**, *5*, 1940–1946.
24. Yoshida, K.; Sato, K.; Anzai, J. Layer-by-layer polyelectrolyte films containing insulin for pH- triggered release. *J. Mater. Chem*. **2010**, *20*, 1546–1552.
25. Becker, A.L.; Johnston, A.P.R.; Caruso, F. Layer-by-layer assembled capsules and films for therapeutic delivery. *Small* **2010**, *6*, 1836–1852.
26. Sato, K.; Yoshida, K.; Takahashi, S.; Anzai, J. pH- and sugar-sensitive layer-by-layer films and microcapsules for drug delivery. *Adv. Drug Deliv. Rev.* **2011**, *63*, 809–821.
27. Sato, K.; Takahashi, S.; Anzai, J. Layer-by-layer thin films and microcapsules for biosensors and controlled release. *Anal. Sci*. **2012**, *28*, 929–938.
28. Skirtach, A.G.; Karageorgiev, P.; Bédard, M.F.; Sukhorukov, G.B.; Möhwald, H. Reversibly permeable nanomembranes of polymeric microcapsules. *J. Am. Chem. Soc.* **2008**, *130*, 11572–11573.
29. Farhat, T.R.; Schlenoff, J.B. Ion transport and equilibria in polyelectrolyte multilayers. *Langmuir* **2001**, *17*, 1184–1192.
30. Stoeve, P.; Vasquez, V.; Coelho, M.A.N.; Rabolt, J.F. Gas transfer in supported films made by molecular self-assembly of ionic polymers. *Thin Solid Films* **1996**, *284*, 708–712.
31. Kumar, S.K.; Hong, J.D. Photoresponsive ion gating function of an azobenzene polyelectrolyte multilayer spin-self-assembled on a nanoporous support. *Langmuir* **2008**, *24*, 4190–4193.
32. Kösters, J.; Schönhoff, M.; Stolwijk, N.A. Ion transport effects in a solid electrolyte due to salt substitution and addition using an ion liquid. *J. Phys. Chem. B* **2013**, *117*, 2527–2534.

33. Harris, J.J.; Stair, J.L.; Bruening, M.L. Layered polyelectrolyte films as selective, ultrathin barriers for anion transport. *Chem. Mater.* **2000**, *12*, 1941–1946.
34. Krasemann, L.; Tieke, B. Selective ion transport across self-assembled alternating multilayers of cationic and anionic polyelectrolytes. *Langmuir* **2000**, *16*, 287–290.
35. Toutianoush, A.; Tieke, B. Selective transport and incorporation of highly charged metal and metal complex ions in self-assembled polyelectrolyte multilayer membranes. *Mater. Sci. Eng. C* **2002**, *22*, 135–139.
36. Ono, S.S.; Decher, G. Preparation of ultrathin self-standing polyelectrolyte multilayer membranes at physiological conditions using pH-responsive film segments as sacrificial layers. *Nano Lett.* **2006**, *6*, 592–598.
37. Park, J.; Kim, J.; Lee, S.; Bang, J.; Kim, B.J.; Kim, Y.S.; Cho, J. Free-standing film electronics using photo-crosslinking layer-by-layer assembly. *J. Mater. Chem*. **2009**, *19*, 4488–4490.
38. Sato, K.; Shiba, T.; Anzai, J. Preparation of free-suspended polyelectrolyte multilayer films using an alginate scaffold and their ion permeability. *Mater. Sci. Eng. C* **2012**, *32*, 2649–2653.
39. Zhu, H.; Srivastava, R.; McShane, M.J. Spontaneous loading of positively charged macromolecules into alginate-templated polyelectrolyte microcapsules. *Biomacromolecules* **2005**, *6*, 2221–2228.
40. Dressick, W.J.; Wahl, K.J.; Bassim, N.D.; Stroud, R.M. Divalent-anion salt effects in polyelectrolyte multilayer depositions. *Langmuir* **2012**, *28*, 15831–15843.
41. Pau, P.C.F.; Berg, J.O.; McMillan, W.G. Application of Stokes' law to ions in aqueous solution. *J. Phys. Chem*. **1990**, *94*, 2671–2679.
42. Jin, W.; Toutianoush, A.; Pyrasch, M.; Schnepf, J.; Gottschalk, H.; Rammensee, W.; Tieke, B. Self-assembled films of Prussian Blue and analogues: Structure and Morphology, elemental composition, film growth, and nanosieving of ions. *J. Phys. Chem*. **2003**, *107*, 12062–12070.
43. Tieke, B.; El-Hashani, A.; Toutianoush, A.; Fendt, A. Multilayered films based on macrocyclic polyamines, calixarenes and cyclodextrins and transport properties of the corresponding membranes. *Thin Solid Films* **2008**, *516*, 8814–8820.
44. El-Hashani, A.; Toutianoush, A.; Tieke, B. Layer-by-layer assembled membranes of protonated 18-azacrown-6 and polyvinylsulfonate and their application for highly efficient anion separation. *J. Phys. Chem. B* **2007**, *111*, 8582–8588.
45. Mauser, T.; Déjugnat, C.; Sukhorukov, G.B. Reversible pH-dependent properties of multilayer microcapsules made of weak polyelectrolytes. *Macromol. Rapid Commun*. **2004**, *25*, 1781–1785.